

TWO-DIMENSIONAL NUMERICAL OPTIMIZATION OF MIS SOLAR CELL ON N-TYPE SILICON

S. Vitanov, P. Vitanov*, and V. Palankovski
 AMADEA Group, TU Wien
 Gusshausstr. 27-28, 1040 Vienna, Austria
 *CL SENES, Bulgarian Academy of Sciences,
 Tzarigradsko Chausse 72, Sofia, Bulgaria

ABSTRACT: The studies on metal oxides and mixed system have shown, that some of them form a negative fixed charge at the interface when deposited on silicon substrate. After deposition of dielectric layers with negative fixed charge on p-type silicon substrate an inversion layer is formed, leading to a back surface field for the minority carriers and thereby reducing the surface recombination velocity. The experiments with metal-insulator-semiconductor solar cells on n-type silicon, using $(Al_2O_3)_x(TiO_2)_{1-x}$ as a dielectric with a negative fixed charge are under way. In this paper, our two-dimensional device simulator MINIMOS-NT is applied for the optimization of these novel devices. The impact of various cell parameters, such as the spacing between the contact metal fingers, the substrate resistivity, and the negative fixed charge density on the cell's current-voltage (I-V) characteristics is investigated.

Keywords: Silicon Solar Cell, n-type, Simulation, Optimization, Interfaces

1 INTRODUCTION

Recently, an idea has been put forward to realize a metal-insulator-semiconductor (MIS) solar cell on n-type silicon, using a dielectric with negative fixed charge on the interface with the semiconductor [1-6]. At the Central Laboratory of Solar Energy and New Energy Sources experiments with MIS solar cell, using $(Al_2O_3)_x(TiO_2)_{1-x}$ as a dielectric with a negative fixed charge, are under way. The density of the fixed charge exceeds $6 \times 10^{11} \text{ cm}^{-2}$ [2]. Ag:Al metal contacts are applied by screen printing and self-centered p+ regions are formed beneath them. The inversion layer is in contact with the p+ layer under the metal contacts, which allows collecting the generated minority carriers on the front metal grid. Thus, difficulties concerning the necessary tunnel oxides for MIS solar cells on p-type silicon are avoided, but the problem with inversion layer resistivity remains. The optimization of the spacing between the metal fingers of the contact grid, the substrate-doping concentration, and the density of the fixed charges is essential for realizing high-efficiency solar cells. For that purpose, we use our two-dimensional device simulator MINIMOS-NT [7], which allows to get a good insight into the operation of the new device.

2 SIMULATION DETAILS

2.1 Simulation domain and solar cell parameters

We assume similar geometries for all devices under investigation with two p+ regions below the metal fingers, n-type silicon substrate, and metal electrode on the backside as shown in Fig.1. The front metal contact spacing (s) is varied. The width of the front metal contact fingers is kept constant ($w = 100 \mu\text{m}$). The elementary simulated cell is given by the substrate thickness and surface area $(s + w) dz$, where $dz = 100 \mu\text{m}$ is the length of the third dimension. In order to minimize computational time, we limit our two-dimensional simulation setup to such an elementary cell (see Fig.1). Table I summarizes the most important design parameters of the solar cells under investigation.

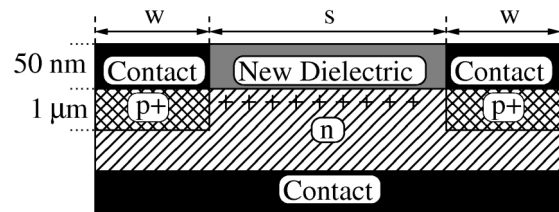


Figure 1: Schematic layer structure of the elementary cells under investigation.

Table I: Simulation parameters.

Cell structure	MIS solar cell with local p+ regions
Substrate	n-type silicon, variable doping level
Cell thickness	330 μm
p++ diffusion	$N_A = 2 \times 10^{19}$, depth = 1 μm
Front grid	parallel metal (Ag:Al) fingers, front finger spacing 500 μm , 250 μm , and 150 μm
Back contact	full back surface metallization
Illumination	intensity of 100 mW/cm^2 , monochromatic light at wavelength of 800 nm
Reflection	roughly 10 %
Contact resistance	neglected
Temperature	300 K
SRH bulk recombination	midgap traps with $N_t = 1 \times 10^{17}$, a doping-level dependence of the SRH minority carrier lifetime
Auger recombination	$C_n = 2.8 \times 10^{-31}$, $C_p = 9.9 \times 10^{-32}$ at 300 K
Surface recombination	front side with dielectric midgap traps, $S_n = S_p = 1000 \text{ cm/s}$

In this work, we use our numerical two-dimensional device simulator MINIMOS-NT [7]. It allows a good control of the size of the simulation grid, which is essential for the simulation of comparatively large devices, such as silicon solar cells [8]. Under the assumption of low-injection condition in the silicon substrate (base), the Poisson equation and the current continuity equations for the minority and majority carriers are solved self-consistently (drift-diffusion transport model). Shockley-Read-Hall (SRH) bulk and surface recombination, Auger recombination, doping-dependent carrier mobility, and optical generation are accounted for. The surface recombination velocity at the front side is 1000 cm/s. Exposure to monochromatic light at wavelength 800 nm and intensity of 100 mW/cm² is simulated. Since the device simulation tool does not support textured surface and antireflection coating, the front surface is assumed to be planar with reflection losses of roughly 10%.

A negative fixed charge with density $D_{ox} = 6 \times 10^{11}$ cm⁻² on the dielectric/silicon interface creates a strong inversion at the silicon surface. The inversion layer is in contact with the p+ diffusion regions, which allows the generated minority carriers in silicon substrate to be collected by the front-side metal grid. The full current-voltage (I-V) curve of the illuminated MIS solar cell is simulated. Thus, the use of simplifying assumption for the cell fill factor (and efficiency) can be avoided. The effect of the spacing between metal fingers, substrate doping concentration, and density of negative fixed charge were investigated.

2.2 Effect of metal contact spacing

Fig. 2 shows the dependence of the non-ideal I-V curve on the contact spacing s . For the simulation illumination with monochromatic light (wavelength 800 nm and intensity 100 mW/cm²) is used. The n+ doping concentration is $N_D = 1 \times 10^{15}$ cm⁻³ and negative fixed charge density is 6×10^{11} cm⁻². Table II summarizes the short-current density (J_{isc}) results, only when the illuminated front surface between the contacts of the elementary cell is accounted for.

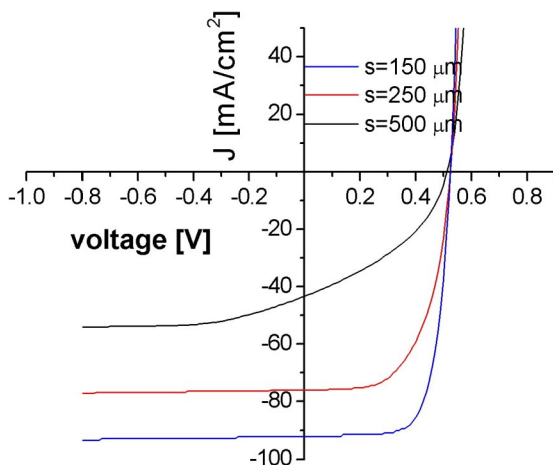


Figure 2: I-V curves of MIS solar cells with different contact spacing s .

Table II: Simulation results for various s .

Metal Contacts spacing s [μm]	J_{osc} [mA/cm ²]	J_{TSC} [mA/cm ²]	V_{oc} [V]	FF
500	43.6	36.3	0.51	0.39
250	76.0	54.3	0.52	0.60
100	91.9	55.2	0.52	0.71

Using the two-dimensional simulation results for the contribution of the inversion layer to the total series resistance, the fill factor was calculated from a conventional expression. We observe a considerable reduction in the cell fill factor with the increase of the spacing between the metal contacts. This is caused by the resistive losses due to the lateral flow of optically-generated carriers in the inversion layer [9].

2.2 Impact of negative fixed oxide charge

The negative fixed charge density defines the concentration of the minority carriers in the inversion layer, thereby its resistivity. Compared to p-type MIS cells the mobility of minority carriers is two times lower. In order to study the effect of resistivity losses in the inversion layer, simulations with three different values of D_{ox} (3×10^{11} , 9×10^{11} , and 1.2×10^{12} cm⁻²) are performed. All other physical parameters are kept the same. Fig. 3 shows the results for $s = 250$ μm .

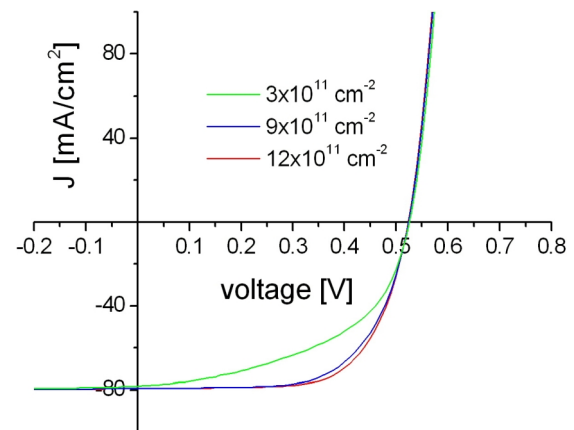


Figure 3: Dependence of the I-V characteristics on the negative fixed oxide charge density.

The short-circuit current I_{sc} and open circuit voltage V_{oc} stay constant. The fill factor (FF) decreases for $D_{ox} = 3 \times 10^{11}$ cm⁻². The effect is at least pronounced for $s = 150$ μm . For $D_{ox} > 6 \times 10^{11}$ cm⁻² there is no considerable difference in FF, due to the insignificant change in the surface potential, thus also unchanged sheet conductivity of the inversion layer. Fig. 4 shows the hole current density distribution for $D_{ox} = 6 \times 10^{11}$ cm⁻² and $s = 250$.

2.2 Impact of doping concentration of the silicon substrate

Full I-V characteristics for the cell with $s = 250$ μm and $D_{ox} = 6 \times 10^{11}$ cm⁻² and several values of N_D are

simulated: $1 \times 10^{16} \text{ cm}^{-3}$ ($0.5 \text{ } \Omega \cdot \text{cm}$), $5 \times 10^{15} \text{ cm}^{-3}$ ($1 \text{ } \Omega \cdot \text{cm}$), $9 \times 10^{14} \text{ cm}^{-3}$ ($5 \text{ } \Omega \cdot \text{cm}$), $4 \times 10^{14} \text{ cm}^{-3}$ ($10 \text{ } \Omega \cdot \text{cm}$), $2 \times 10^{14} \text{ cm}^{-3}$ ($20 \text{ } \Omega \cdot \text{cm}$), and $8 \times 10^{13} \text{ cm}^{-3}$ ($50 \text{ } \Omega \cdot \text{cm}$). The results are summarized in Table III.

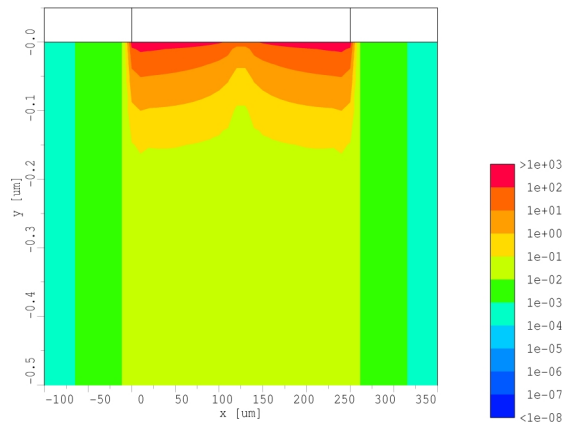


Figure 4: Hole current density distribution under the top surface.

Table III: Simulation results for various N_D .

N_D [cm^{-3}]	J_{TSC} [mA/cm^2]	V_{OC} [V]	FF
1×10^{16}	52.83	0.578	0.55
5×10^{15}	53.43	0.565	0.57
9×10^{14}	55.14	0.525	0.59
4×10^{14}	56.37	0.505	0.58
2×10^{14}	57.29	0.495	0.56
8×10^{13}	60.23	0.475	0.48

With decreasing doping concentration N_D , the short circuit current increases slightly, but V_{oc} and the fill factor decrease.

3 SIMULATION OF SPECTRAL RESPONSE

Fig. 5 shows the relative spectral response as a function of photon energy. The response begins at the bandgap energy and reaches a peak at around 2.1 eV. The lack of nanosecond lifetime “dead layers” in the heavily-doped diffused regions improves the response at high photon energies.

4 CONCLUSION

In this work, our two-dimensional device simulator MINIMOS-NT is used to investigate the behavior of novel MIS solar cells. The impact of various parameters: substrate resistivity, oxide charges, and spacing between the metal contacts is studied. The spectral response is modeled. The results demonstrate some advantages of MIS solar cells on n-type silicon. The numerical simulation analysis shows that by optimizing the device design and physical parameters, a good efficiency can be achieved.

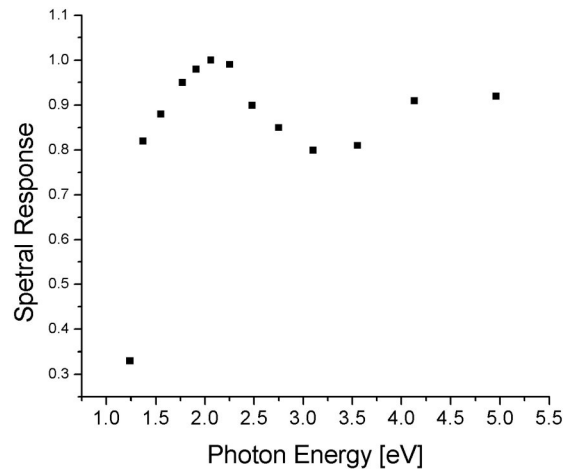


Figure 5: Relative spectral response of MIS n-type Si solar cell.

ACKNOWLEDGEMENT

S. Vitanov and V. Palankovski acknowledge support from the Austrian Science Funds (FWF), project START Y247-N13. P. Vitanov acknowledges support from the project grant TN-1504 from the Ministry of Education and Science, Bulgaria.

REFERENCES

- [1] P. Vitanov, A. Harizanova, T. Ivanova, and K. Ivanova, *J. Material Science: Materials in Electronics* 14 (2003) 757.
- [2] P. Vitanov, A. Harizanova, T. Ivanova, Z. Alexieva and G. Agostinelli, *Jap. J. Appl. Phys.* 47 (2006) 5894.
- [3] P. Vitanov, N. Le Quang, O. Court, G. Goer, A. Harizanova, and T. Ivanova, in Proc. 20th European Photovoltaic Solar Energy Conference, (2005).
- [4] P. Vitanov, G. Agostinelli, A. Harizanova, T. Ivanova, M. Vukudinovic, N. Lee Quang, G. Beaucarne, *Solar Energy Materials and Solar Cells* 90 (2006) 2489.
- [5] G. Agostinelli, A. Delabie, P. Vitanov, Z. Alexieva, H.F.W. Dekkers, S. de Wolf, and G. Beaucarne, *Solar Energy Materials and Solar Cells*, 90 (2006) 3438.
- [6] P. Vitanov, A. Harizanova, Patent Application BG N= 109881, 29.05.2007.
- [7] Minimos-NT Device and Circuit Simulator, User's Guide, Rel. 2.0, <http://www.iue.tuwien.ac.at/mmnt>, 2002.
- [8] P. Vitanov, S. Vitanov, and V. Palankovski, in Proc. 21st European Photovoltaic Solar Energy Conference, (2006) 1475.
- [9] A. Aberle, B. Kuhlmann, *Forschungsverbund Sonnenenergie "Themen 95/96"*, (1996) 103.